Computers and Electronics in Agriculture 160 (2019) 14–22

Contents lists available at ScienceDirect

Computers and Electronics in Agriculture

journal homepage: www.elsevier.com/locate/compag

Original papers

A new spray deposition pattern measurement system based on spectral analysis of a fluorescent tracer

Yao Wen[a,d], Ruirui Zhang[a,d,*], Liping Chen[b,c,*], Yanbo Huang[e], Tongchuan Yi[b,c], Gang Xu[b,c], Longlong Li[b,c], Andrew John Hewitt[f]

[a] Beijing Research Center of Intelligent Equipment for Agriculture, Beijing Academy of Agricultural and Forestry Sciences, Beijing 100097, China
[b] National Research Center of Intelligent Equipment for Agriculture, Beijing 100097, China
[c] National Center for International Research on Agricultural Aerial Application Technology, Beijing 100097, China
[d] Beijing Key Laboratory of Intelligent Equipment Technology for Agriculture, Beijing Academy of Agricultural and Forestry Sciences, Beijing 100097, China
[e] United States Department of Agriculture, Agricultural Research Service, Crop Production Systems Research Unit, PO Box 350, Stoneville, MS 38776, USA
[f] Centre for Pesticide Application and Safety, The University of Queensland, Queensland 4072, Australia

ARTICLE INFO

Keywords:
Aerial spraying
Deposition pattern measurement
Fluorescent tracer
Spectral analysis
Unmanned aerial vehicle

ABSTRACT

To complement shortages of discrete sampling data and improve the detection accuracy of droplet deposition in unmanned aerial vehicle (UAV) spraying, we developed a new spray deposition pattern measurement system (SDPMS) based on a fluorescent tracer and spectral analysis. Then, we evaluated the system performance in two field spraying experiments in comparison with water-sensitive paper results. The system comprises a fluorescence scanner and spectral analysis program. The fluorescence scanner includes an ultraviolet light, spectrometer, far end controller, stepping motor, and sample reel. First, 1.0% fluorescent tracer solution is sprayed, and the droplets are collected on a paper strip. Then, the paper strip is scanned with the fluorescence scanner, and a set of fluorescence intensity values is collected and processed by the spectral analysis program. Finally, the spray deposition pattern is calculated. The experimental results showed that the spray deposition pattern from the SDPMS had a 0.89 correlation coefficient with that of water-sensitive paper. A linear regression model between fluorescence intensity and deposit coverage was constructed, with a coefficient of determination of 0.91 ($F = 61.8845$, $P < 0.001$). In addition, a linear regression model between fluorescence intensity and volume rate was constructed, with a coefficient of determination of 0.89 ($F = 51.6639$, $P < 0.001$). The SDPMS and field experiments offer a good foundation for the development of an improved system compatible with UAV spraying.

1. Introduction

Unmanned aerial vehicle (UAV) chemical spraying is increasingly used for crop protection, as it can increase disease and pest control efficiency while minimizing worker exertion and exposure to chemicals (Xue et al., 2016; He et al., 2017; Morey et al., 2017; Yang et al., 2017; Tang et al., 2018). The spray deposition pattern is one of the most important factors that influences the chemical control effect, which is typically evaluated based on the uniformity of the droplet deposition distribution, droplet coverage, and volume rate (Nuyttens et al., 2007; Dorr et al., 2013; Heidary et al., 2014; Wang et al., 2017).

Many systematic studies of equipment and technology to measure spray deposition patterns have been conducted over the past few decades. One of the most common methods includes the use of water-sensitive paper (WSP) along with traditional optical techniques to analyze images of droplets from spray systems (Zhu et al., 2011; Bae and Koo, 2013; Chen et al., 2016). Moreover, studies have attempted to evaluate the application of fluorescent tracer methods using spectrophotometers for the estimation spray deposition (Wang et al., 2016; Huang et al., 2017). However, the results from WSP lack sufficient accuracy, since the stained areas on the WSP card are readily affected during collection and handling of exposed samples, and fluorescent tracer methods rely on expensive equipment. Furthermore, both methods require complex operations, and are time- and labor-intensive.

Abbreviations: $C_{485–495}$, average spectral value in the band range 485–495 nm on the paper strip; R_C, modeling decision coefficient; SDPMS, spray deposition pattern measurement system; SNV, standard normalized variable; UAV, unmanned aerial vehicle; WSP, water-sensitive paper

* Corresponding authors at: Beijing NongKe Mansion Building, Shuguang Huayuan Middle Road No. 11, Haidian District, Beijing, China.
E-mail addresses: weny@nercita.org.cn (Y. Wen), zhangrr@nercita.org.cn (R. Zhang), chenlp@nercita.org.cn (L. Chen), yanbo.huang@ars.usda.gov (Y. Huang), yitc@nercita.org.cn (T. Yi), xug@nercita.org.cn (G. Xu), lill@nercita.org.cn (L. Li), a.hewitt@uq.edu.au (A.J. Hewitt).

https://doi.org/10.1016/j.compag.2019.03.008
Received 28 November 2018; Received in revised form 28 February 2019; Accepted 7 March 2019
Available online 12 March 2019
0168-1699/

In laboratory settings, more accurate methods rely on laser particle analyzers to measure spray patterns from nozzles to determine droplet size distributions (Tuck et al., 1997; Tang et al., 2016); however, these systems are often too expensive for widespread in-field use. There have been several recent developments to measure spray application and droplet distribution using electronic sensing platforms (Salyani and Serdynski (1990); Zhang et al., 2014; Melissa et al., 2015; Xu et al., 2015) and other methods (e.g., remote sensing, infrared thermography, etc.; Zhang et al., 2012; Zhang et al., 2016). The detection accuracy of such systems has been assessed using data processing methods and the resolution of the electronic sensor, but the reliability of these systems remains questionable.

To address these limitations, we designed a new spray deposition pattern measurement system (SDPMS) based on spectral analysis and fluorescence tracing (Zhang et al., 2017), which we tested by measuring the spray deposition pattern of a quadrotor UAV equipped with a spraying system. Finally, the correlation between the spray deposition pattern from the SDPMS and droplet deposition parameters from the WSP was analyzed with a linear regression model of the deposition pattern.

2. Development of the SDPMS

2.1. Underlying principle

Fluorescent compounds absorb light or other electromagnetic radiation energy and emit photons to return to their ground state while simultaneously emitting fluorescence, which can be measured by detectors (Fig. 1). Fig. 1 presents a schematic of the principle underlying fluorescence measurements.

Several parameters influence the intensity and shape of the spectrum of fluorescent compounds, and the fluorescence intensity of the fluorescent substance (lx) F can be expressed as Eq. (1):

$$F = f\left(\rho, \frac{S_1+\ldots+S_n}{S}, E\right) \quad (1)$$

where f is the formula symbol, ρ represents the mass fraction of the fluorescent compound (%), S represents the sampling area of the fluorescence measurement (mm^2), S_1, $S_2 \ldots S_n$ are the coverage area of each fluorescent compound (mm^2), and E represents the intensity of the source light (lx).

Among fluorescent compounds, RQT-C-3 is a fluorescent brightener with a strong fluorescent signal, which is used in waterborne coatings and is readily water soluble. Given these advantages, we selected it as the fluorescent tracer for the SDPMS spraying experiment. The fluorescent tracer solution was mixed with water to a final mass concentration of 1.0%, and ultraviolet light with a central wavelength of 365 nm was applied to excite RQT-C-3. Under ideal conditions at such a concentration, there is a linear relationship f between the fluorescence intensity and coverage of the fluorescent tracer. Thus, the volume rate of the fluorescent tracer could also be calculated based on the coverage.

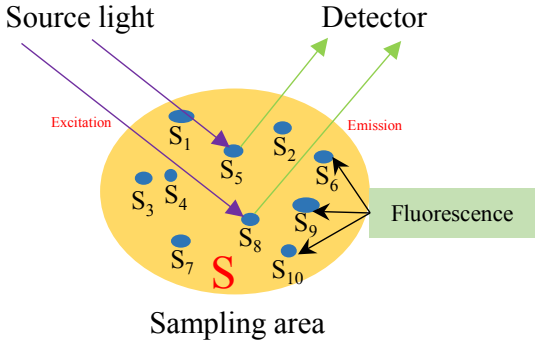

Fig. 1. Fluorescence measurement scheme. S, sampling area of the fluorescence measurement; S_1, $S_2 \ldots S_{10}$, coverage area of each fluorescent compound.

Fig. 2 presents a schematic diagram of the SDPMS applied to UAV spraying. Fluorescent tracer solution at a 1.0% mass concentration was sprayed by a quadrotor UAV, and a paper strip was placed in the flight direction to collect the droplets. Finally, the fluorescence intensity of the tracer on the paper could be detected, and the deposition pattern calculated, by the SDPMS.

2.2. System design

The SDPMS comprises a fluorescence scanner and spectral analysis program, run on a tablet PC. The fluorescence scanner is connected to the tablet PC via a universal serial bus (USB) connection. Fig. 3 illustrates the general structure of the SDPMS.

The fluorescence scanner includes a spectrometer, far end controller, stepping motor, sample reel, paper strip, ultraviolet light, and photoelectric switch. The paper strip is wound onto the sample reel, and a two-phase hybrid stepping motor is used to drive the shafts of the sample reel. A far end controller is connected to the stepping motor, ultraviolet light, and photoelectric switch. The spectrum on the paper strip is collected and sent to the spectral analysis program via the spectrometer. The components of the SDPMS are shown in Fig. 4.

A miniature FLAME-S-VIS-NIR spectrometer (resolution: 2048 pixels, effective wavelength range: 340–1014 nm; Ocean Optics, Dunedin, FL, USA) covering the excitation and emission wavelengths of the fluorescent tracer was used as the core component of the system. The spectrometer open bench is shown in Fig. 5. The light from the detected compound enters the optical bench through the fiber optic connector, provides a precise location for the end of the optical fiber, slit, and absorbing filter. Then light passes through the slit, installed so as to achieve a suitable optical resolution. An absorbing filter is installed between the slit and the aperture in the fiber optic connector to limit the bandwidth of light entering the spectrometer. Light reflects from this collimating mirror, which reduces the effects of excitation scattering on the fluorescence measurements. In addition, specific grating is installed on the platform to select the preferred wavelength range and eliminate mechanical shifts or drift. First-order spectra on the detector plane are focused using a focusing mirror to guarantee the highest reflectance and lowest stray light possible. A detector collection lens is fixed to the detector to focus the light from the tall slit onto the shorter detector elements, which can increase the light collection efficiency and reduce stray light. A Sony ILX511B linear CCD array was adopted as the detector, which responds to the wavelength of light striking each pixel and outputs an analog signal from each pixel that is converted via an analog–digital converter into a digital signal. The driver electronics process this signal and send the spectrum via the USB connection to the PC software. Finally, an order-sorting filter is used to block second- and third-order light from reaching specific detector elements to increase the accuracy of the spectrometer response.

The system uses an 8051 series microcontroller (version STC12C5410AD; STCmicro, China) for the far end controller control. The rotating speed of the stepping motor is 30 r min^{-1}. An 80-mm-diameter reel was constructed as the sampling reel. Based on these parameters, the microcontroller of the far end controller converts the rotation count of the stepping motor to a linear distance L (m) of the sample reel using Eq. (2):

$$L = \frac{40\pi t + 0.15t^2}{1000} \quad (2)$$

where t is the sampling time (s).

A kraft paper strip (width: 19.3 mm, thickness: 0.3 mm) is used that contains no fluorescent compounds itself, and exhibits a degree of water absorbability and suitable robustness for the SDPMS. A photoelectric switch (sensing distance: < 5 cm, response frequency: 200 Hz) is used to detect opaque objects and provide corresponding instructions for the far end controller to switch the spectrum acquisition on and off.

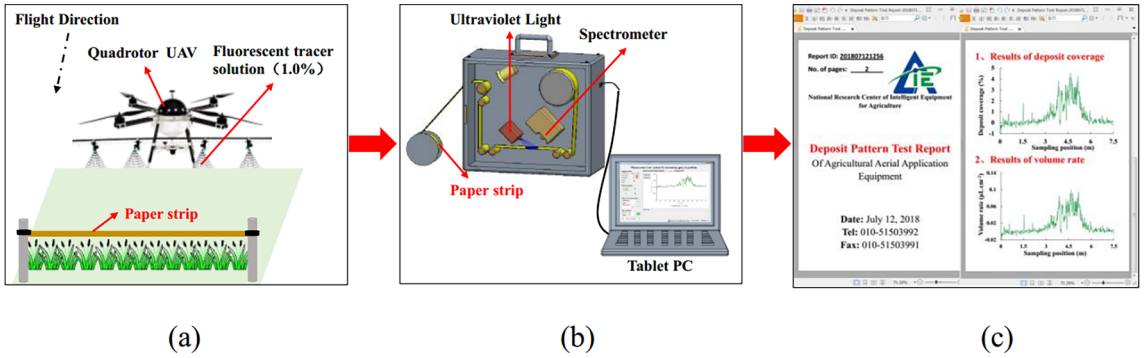

Fig. 2. Schematic diagram of the SDPMS using a UAV spray application: (a) field experiment, (b) SDPMS, and (c) deposition pattern reports.

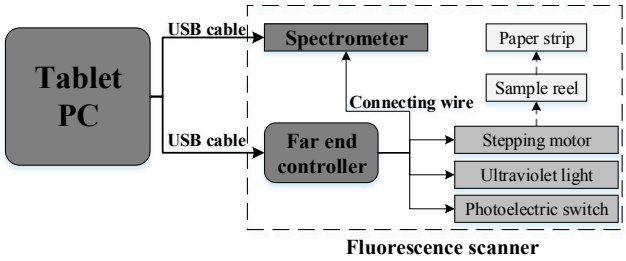

Fig. 3. General structure of the SDPMS.

In tandem with the fluorescence detector, we developed a spectral analysis program for spray deposition pattern measurement, coded using the C# language on the Visual Studio 2015 platform (Microsoft Corp., Redmond, WA, USA). The program enables communication with the fluorescence scanner, acquisition parameter settings, spectral acquisition control, spectrum processing and analysis, and generation of the deposition pattern. The deposition pattern is described in a two-dimensional line chart, which shows the changes in fluorescence intensity along with the sampling position. The deposition pattern can be viewed on the program interface and is stored as a CSV file. By user request, historical deposition patterns can be imported and viewed on the program interface. The interface of the spectral analysis program is shown in Fig. 6 and a flowchart of the spectral analysis program is shown in Fig. 7.

2.3. Spectral modeling of the deposition pattern

The spectral model functions to preprocess and characterize the spectrum. The preprocessing methods used herein mainly include spectrum smoothing and normalization. The characteristic analysis aims to select the characteristic wave bands of the fluorescence spectrum.

The original fluorescence spectrum of the paper strip obtained by the spectral analysis program contains not only valid information of the sampling position, but also interference components, such as instrument noise and stray light. Spectrum smoothing is used to reduce random noise in the spectrum. The spectrum is smoothed in the spectral analysis program using the Savitzky–Golay convolution algorithm (Hou et al., 2015; Long et al., 2015), which smooths a signal locally with a low-degree polynomial based on the linear least squares method to a sliding window of data. The degree of the polynomial and the length of the sliding window are respectively set to 2 and 15 to improve the reliability of the smoothed spectrum available for analysis.

Then, the smoothed spectrum is normalized by setting the absorbance value of each wavelength point in the spectrum to satisfy a certain distribution (i.e., normal distribution) to eliminate the influences of the linear translation of the spectrum. Each spectrum of the sampling position is corrected by the spectral analysis program using the standard normalized variable (SNV) algorithm (Li, 2006; Fearn et al., 2009; Guo et al., 2016). The standard normalized intensity of spectrum Z_i can be calculated using Eq. (3):

$$Z_i = \frac{x_i - \mu}{\sigma} \tag{3}$$

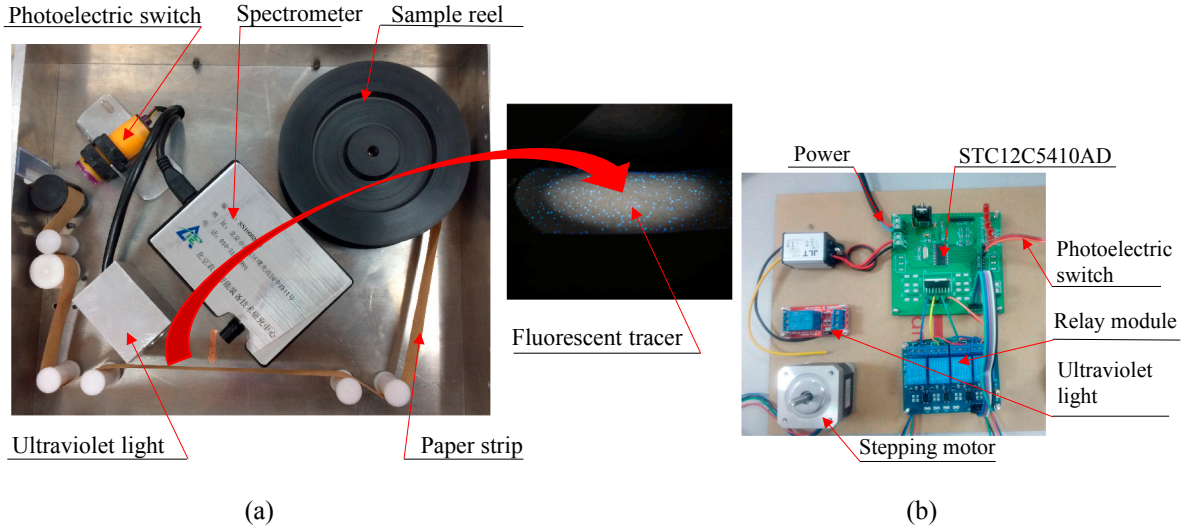

Fig. 4. Fluorescence scanner components of the SDPMS: (a) device structure; (b) hardware connection.

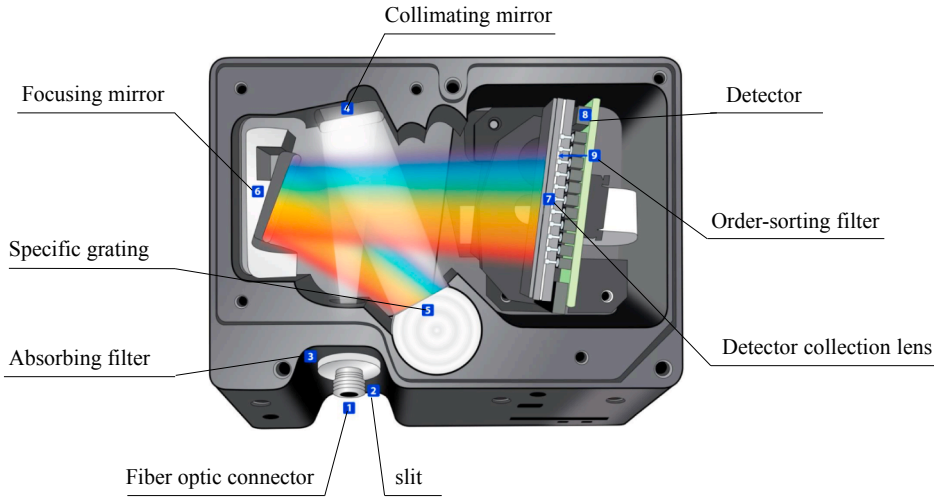

Fig. 5. Spectrometer open bench.

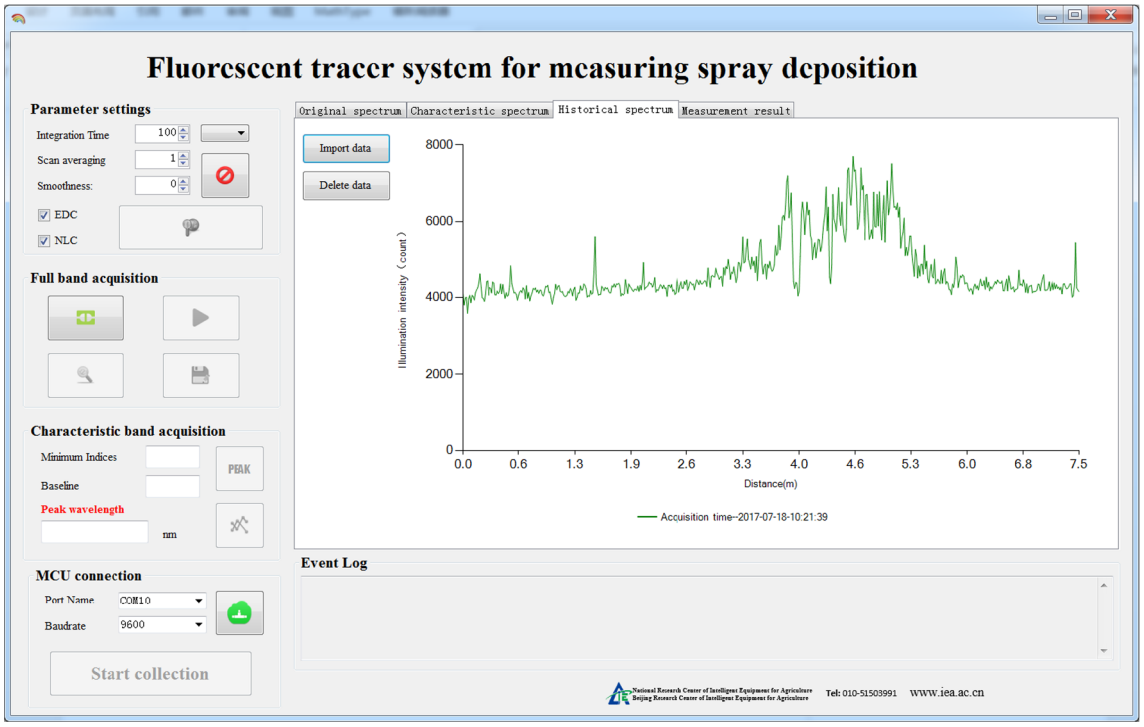

Fig. 6. Spectral analysis program interface.

where x_i is the raw intensity of spectrum (lx), μ is the mean value (lx) and σ is the standard deviation (lx).

Fig. 8 presents the typical spectra of four sampling positions on the paper strip after spectrum preprocessing with the smoothing and normalization algorithm. The characteristics of the spectra indicated that ultraviolet light information was collected, based on the fluorescence excitation during spectrum acquisition and the saturation of fluorescence intensity in the band range of 340–400 nm. Therefore, the band range of 400–1014 nm was extracted for the characteristic analysis. The spectra exhibited a peak near the spectral band of 490 nm, and the band range of 485–495 nm was selected for subsequent characteristic analysis.

3. Field experiment

A field experiment (Fig. 9) was designed to evaluate the performance of the SDPMS. It was performed on July 16, 2017, in a cotton field in Xinjiang Province, China (44°26′18.0552″N, 85°40′46.5050″W), using a quadrotor UAV (XAIRCRAFT, Guangzhou, China) equipped with a rotary atomizer. The cotton canopy height was 0.8–1.2 m, and the paper strip was mounted on a shelf at a height of 1 m above the ground. The main conditions and parameters of the two tests are shown in Table 1.

One of the most common methods for analyzing spray deposition patterns includes the use of WSP and digital image processing techniques to analyze images of sprayed droplets (Fox et al., 2003, Zhou and He, 2016). WSP is a type of rigid paper coated with the chemical indicator bromophenol blue, which changes from yellow to blue after contact with droplets. The number and deposition of droplets per centimeter squared (assuming that the droplets are spherical in the air), the percent coverage, volume median diameter, and number median diameter can be extracted from the WSP digital image by image processing software, such as ImageJ, DepositScan, etc. To quantify the deposit coverage and volume rate, WSP (26 mm × 76 mm; Syngenta

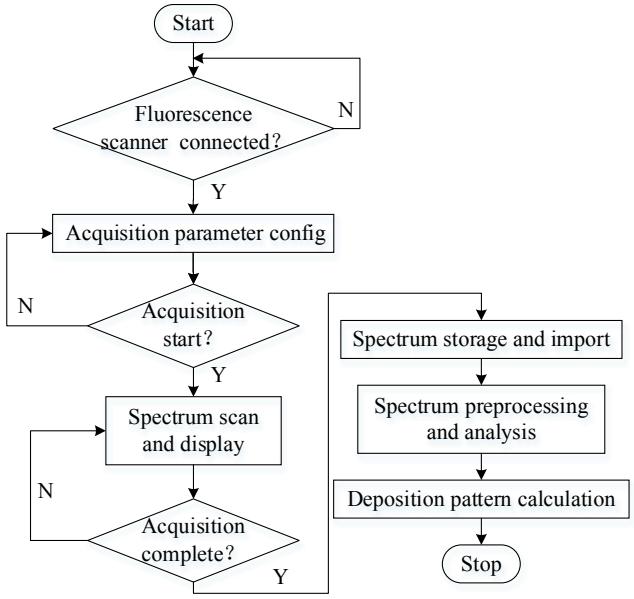

Fig. 7. Flowchart of the spectral analysis program.

Crop Protection AG, Switzerland) was placed near the paper strip (Fig. 9(b)). To cover the effective swath, the sample length of the paper strip was set to 7 m. In total, 15 WSP cards evenly spaced 0.5 m apart were placed along with the paper strip, which were labeled W1-1 to W1-15 (test #1) or W2-1 to W2-15 (test #2). After each spraying, the paper strip and WSP cards were collected immediately and stored in separate sealed bags.

The paper strips from the two tests were each scanned with the SDPMS, with an integration time of the spectrometer and scanning time interval of 100 ms. To compare the WSP and SDPMS measurement results, the spectra of three sampling points were selected on the paper strip near each corresponding WSP card. The spectral average values of the three sampling positions were calculated and taken as the measurement spectrum of each sampling position. In total, 15 sampling positions were selected on the paper strip of each test. The measurement results from the 15 sampling positions were denoted as S1-1 to S1-15 (test #1) or S2-1 to S2-15 (test #2). Finally, the averages of 15 spectra from each paper strip in the two tests were obtained for comparison with the WSP measurement results.

The average spectra in the band range of 420–620 nm shown in Fig. 10 were selected to demonstrate the effect of the spectrum preprocessing method. Fig. 11 shows the results after Savitzky–Golay smoothing. The smoothing algorithm effectively removed noise from the spectra, and the valid spectral information was effectively preserved in the smoothed spectra.

Normalized spectra were obtained with the SNV algorithm (Fig. 12), which resulted in standard normalization of the spectra and effective correction of the spectral differences caused by scattering between sampling positions.

The spectra of the paper strip were processed with the Savitzky–Golay and SNV correction algorithm (Fig. 13). The spectral changes of sampling positions S1-1 to S1-15 and S2-1 to S2-15 were similar. The average spectral value in the band range 485–495 nm of the paper strip sampling position was noted as $C_{485–495}$. It was calculated in spectral analysis program of the SDPMS, and was used to model the deposition pattern. The deposition pattern results of the two tests are shown in Fig. 14.

4. Results and discussion

4.1. WSP data collection and analysis

The WSP cards were scanned into digital images with a high pixel resolution (1200 dpi × 1200 dpi) using a portable scanner (Fig. 15(a)). In addition, fluorescence images of the paper strips in each sample position were captured with a CCD camera (pixel resolution: 1280 pixels × 960 pixels) (Fig. 15(b)). From these images, the droplet deposition parameters, including deposit coverage and volume rate, were calculated using DepositScan software (USDA-ARS, Wooster, OH, USA), which can rapidly evaluate the spray deposit distribution on WSP. Deposit coverage represents the proportion of the stained area covered by droplets to the total area of the WSP cards. Assuming the droplets to be spheres in the air, the volume rate is the volume of deposition points per unit area, which is calculated according to the diameter of the droplet-stained area and the spread factor of the WSP. Fig. 16 presents a comparison of the deposition pattern results from the SDPMS and droplet deposition parameters from the WSP in test #1.

From the comparison, the deposition pattern results measured with the SDPMS were consistent with droplet deposition parameters from the WSP cards. From the correlation analysis, the correlation coefficients of $C_{485–495}$ with the droplet deposition parameters, deposit coverage and volume rate, were 0.91 ($P < 0.01$) and 0.89 ($P < 0.01$), respectively. These results indicate a significant correlation between $C_{485–495}$ and the droplet deposition parameters.

4.2. Modeling the droplet deposition pattern

A linear regression model was constructed based on the spectral average $C_{485–495}$ values and measurement results from the WSP. The predicted values of deposit coverage and volume rate were represented as y_1 and y_2, respectively. The spectral average $C_{485–495}$ values were represented as x. The modeling decision coefficient and the validation

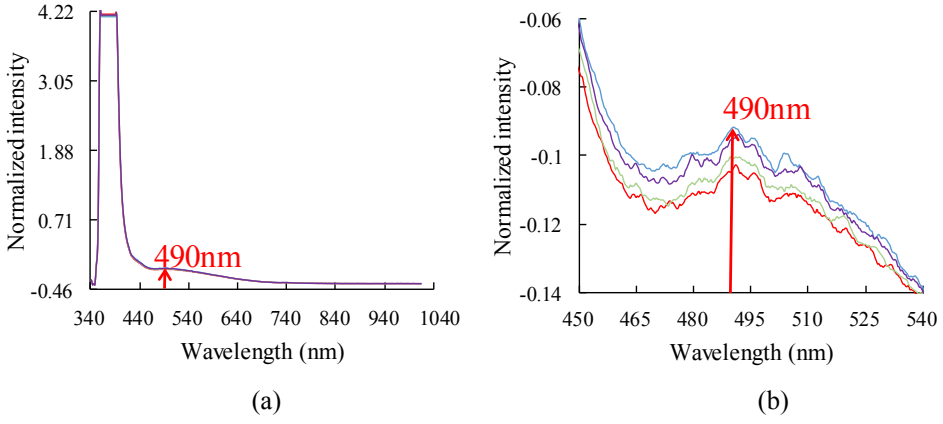

Fig. 8. Spectra at four paper strip sampling positions: (a) whole spectrum; (b) peak near the spectral band of 490 nm.

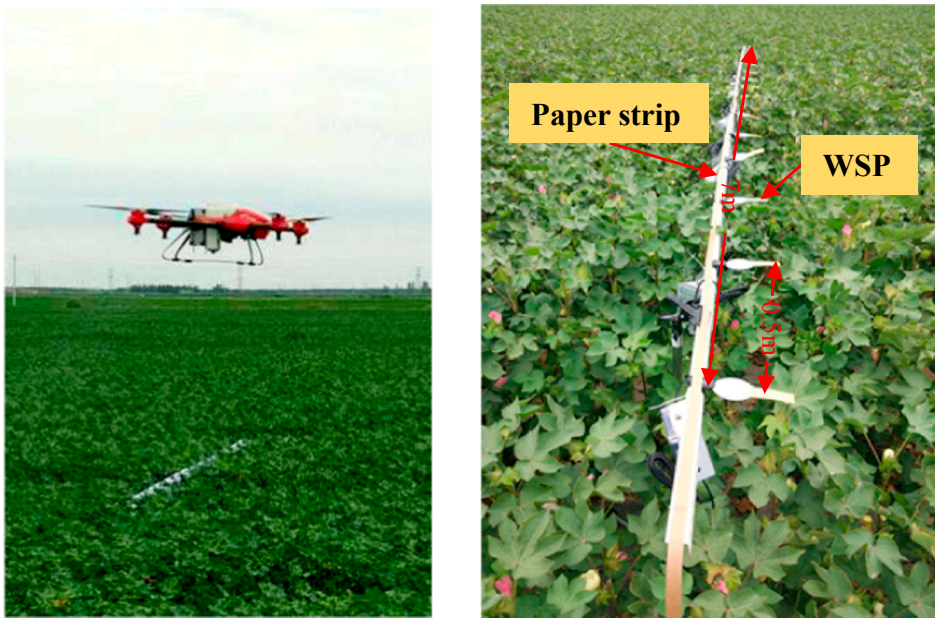

Fig. 9. Field experiment: (a) UAV with a rotary atomizer; (b) layout of the paper strip and WSP.

Table 1
Main parameters of the field tests.

Test	Temperature (°)	Wind speed (m s^{-1})	Humidity (%)	Flight height (m)	Flight speed (m s^{-1})	Effective swath (m)	Application rate (L ha^{-1})
#1	27.8	0	46.5	3	4	3	9.0
#2	26.1	0.2	50.2	3	5	3	9.0

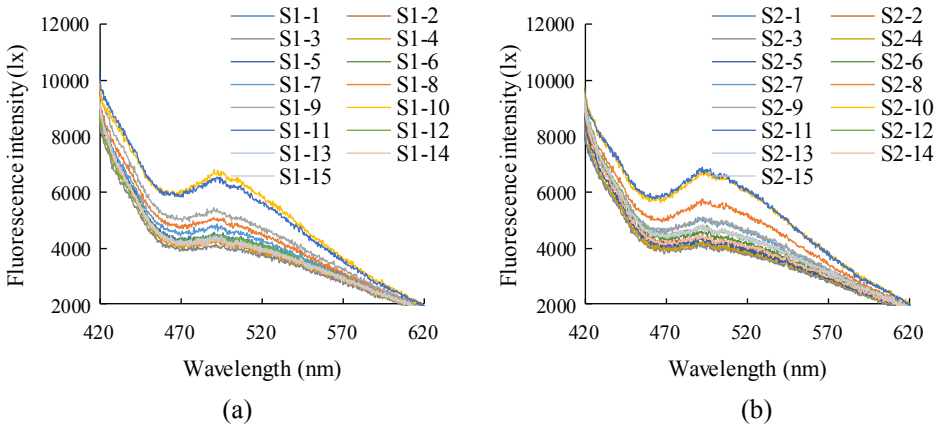

Fig. 10. Average spectra from the paper strip in test (a) #1 and (b) #2.

decision coefficient were represented as R_C and R_V, respectively.

The data from test #1, S1-1 to S1-15 and W1-1 to W1-15, were used to construct the linear regression models, expressed as Eqs. (4) and (5):

$$y_1 = -2.5997 + 25.0747x,\ R_C = 0.91 \quad (4)$$

$$y_2 = 0.0633 + 0.6117x,\ R_C = 0.89 \quad (5)$$

The data of test #2, S2-1 to S2-15 and W2-1 to W2-15, were used to validate the models. Fig. 17 presents a comparison of the test #2 results from the SDPMS and WSP. The R_V values for Eqs. (4) and (5) were 0.93 and 0.89, respectively. These results indicate that the SDPMS has the potential to replace traditional WSP-based methods to more accurately assess spray deposition patterns.

5. Conclusions and future work

We developed a SDPMS comprising a fluorescence scanner and spectral analysis program based on a spectral analysis and fluorescent tracer method. This instrument provides a new tool for the rapid mapping of spray deposition patterns from UAV spraying. The main components of the fluorescence scanner are an ultraviolet light, spectrometer, far end controller, stepping motor, and sample reel. In addition, a paper strip collects the spray droplets and is scanned by the fluorescence scanner. A set of fluorescence intensity values from the paper strip are collected and preprocessed by the spectral analysis program to ultimately calculate the spray deposition pattern.

We performed a field experiment to evaluate the performance of the

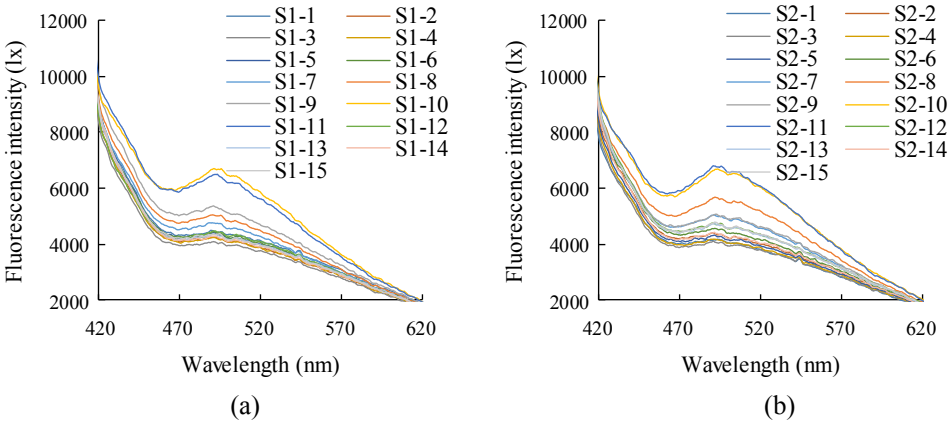

Fig. 11. Savitzky–Golay-smoothed spectra in test (a) #1 and (b) #2.

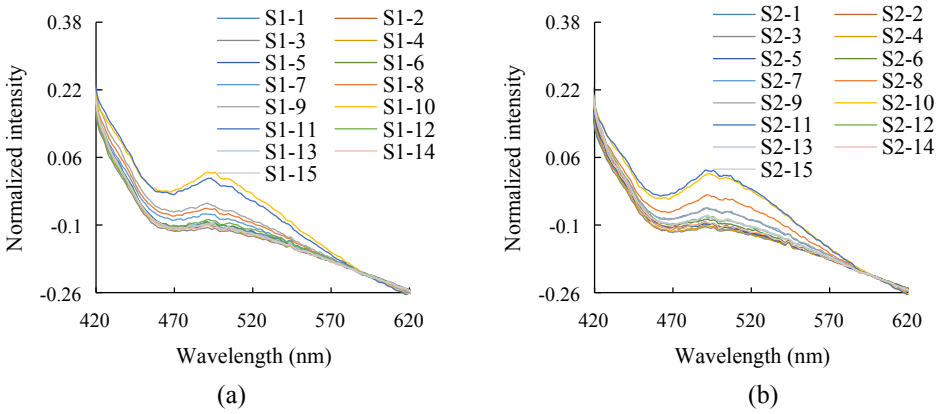

Fig. 12. Spectra after SNV correction in test (a) #1 and (b) #2.

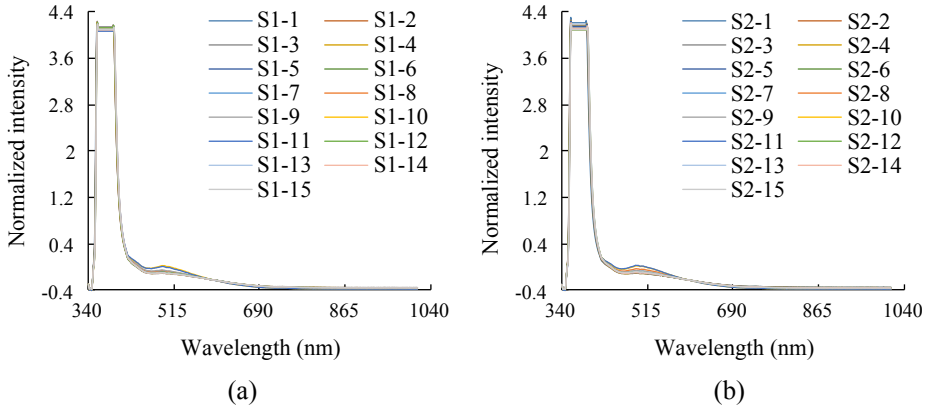

Fig. 13. Saturation of the fluorescence intensity in the whole spectrum in tests (a) #1 and (b) #2.

SDPMS. The linear regression model between the fluorescence intensity from the SDPMS and the measurement results from WSP had high validation coefficients > 0.89.

Although the SDPMS is still a prototype, it represents a new method to measure spray deposition patterns in a rapid and continuous manner, and can satisfy the conditions of UAV spraying, which is widely applied for crop protection but can result in a great spatial difference in deposit distribution due to downwash flow of the rotor. Moreover, the developed method complements the shortages of discrete sampling and can improve the detection accuracy of droplet deposition during UAV spraying when many sampling positions on the paper strip are scanned by the SDPMS. However, there are several limitations of the SDPMS that remain to be resolved. First, the development cost of the SDPMS is comparatively high, considering that the core component of the SDPMS is a commercial spectrometer. The effective wavelength range of this commercial spectrometer is 340–1014 nm, which yields redundant spectral information; therefore, a spectrometer containing only the emission wavelength required for the specific fluorescent tracer will be

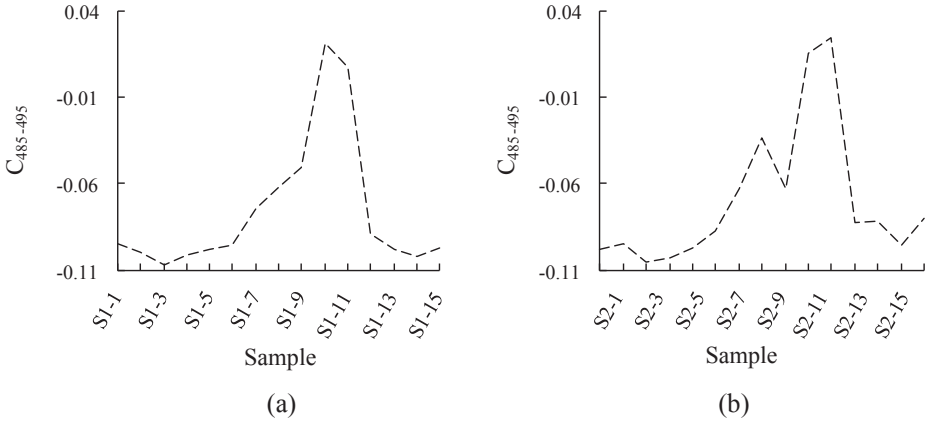

Fig. 14. Deposition pattern results from the SDPMS in tests (a) #1 and (b) #2.

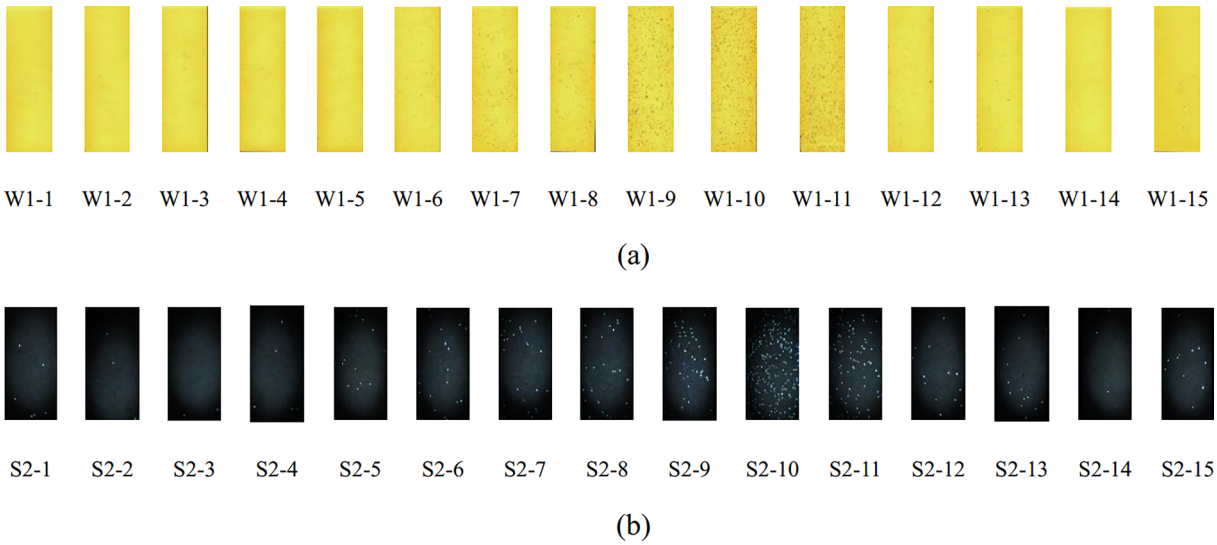

Fig. 15. Images of the results of test #1: (a) WSP images scanned with a portable scanner; (b) fluorescence images of paper strips photographed with a CCD camera.

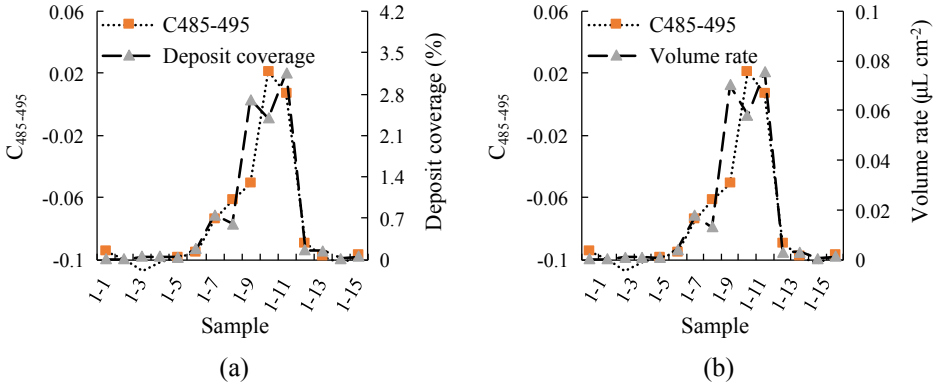

Fig. 16. Comparison of the deposition pattern results from the SDPMS and droplet deposition parameters of the WSP in test #1: (a) deposit coverage; (b) volume rate.

adopted in future versions of the SDPMS to reduce costs. Second, further experiments are needed (and pending) to optimize the spray deposition pattern model, considering as many influencing factors (e.g., spread factor of the fluorescent tracer solution on the paper strip, solution concentration, droplet size, etc.) as possible. Finally, the emission wavelengths of the fluorescent tracer mixed with solutions of aerially applied pesticides remain uncertain; therefore, additional experiments are required to study the influences of sprayed chemicals on the excitation and emission wavelengths of the fluorescent tracer. Regardless of these limitations, the SDPMS prototype presented herein and associated field experiment results offer a good foundation for the development of an improved system compatible with UAV spraying.

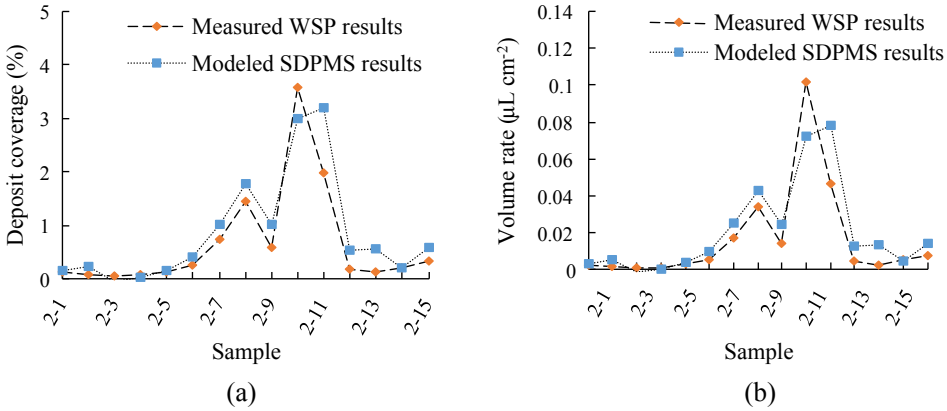

Fig. 17. Comparison of the SDPMS and WSP results from test #2: (a) deposit coverage; (b) volume rate.

Acknowledgments

This research was funded in part by the National Key R&D Program of China (2016YFD0200701-2), Zhang Ruirui's Beijing Nova Program (Z181100006218029), BAAFS Innovation Ability Construction Program 2018 (KJCX20180424), and The National Natural Science Foundation of China (31601228).

Appendix A. Supplementary material

Supplementary data to this article can be found online at https://doi.org/10.1016/j.compag.2019.03.008.

References

Bae, Y., Koo, Y.M., 2013. Flight attitudes and spray patterns of a roll-balanced agricultural unmanned helicopter. Appl. Eng. Agric. 29 (5), 675–682.
Chen, S.D., Lan, Y.B., Li, J.Y., Zhou, Z., Jin, J., Liu, A., 2016. Effect of spray parameters of small unmanned helicopter on distribution regularity of droplet deposition in hybrid rice canopy. Trans. CSAE 32 (17), 40–46.
Dorr, G.J., Hewitt, A.J., Adkins, S.W., Hanan, J., Zhang, H.C., Noller, B.N., 2013. A comparison of initial spray characteristics produced by agricultural nozzles. Crop Prot. 53 (11), 109–117.
Fearn, T., Riccioli, C., Garrido-Varo, A., Guerrero Ginel, J.E., 2009. On the geometry of SNV and MSC. Chemom. Intell. Lab. Syst. 96 (1), 22–26.
Fox, R.D., Derksen, R.C., Cooper, J.A., Krause, C.R., Ozkan, H.E., 2003. Visual and image system measurement of spray deposits using water sensitive paper. Appl. Eng. Agric. 19 (5), 549–552.
Guo, Y., Ni, Y.N., Kokot, S., 2016. Evaluation of chemical components and properties of the jujube fruit using near infrared spectroscopy and chemometrics. Spectrochim. Acta A Mol. Biomol. Spectrosc. 153, 79–86.
He, X.K., Bonds, J., Herbst, A., Langenakens, J., 2017. Recent development of unmanned aerial vehicle for plant protection in East Asia. Int. J. Agric. Biol. Eng. 10 (3), 18–30.
Heidary, M.A., Douzals, J.P., Sinfort, C., Vallet, A., 2014. Influence of spray characteristics on potential spray drift of field crop sprayers: a literature review. Crop Prot. 63 (5), 120–130.
Hou, P.G., Li, N., Chang, J., Wang, S.T., Song, T., 2015. Research on analysis of oil in water based on the joint optimization of Savitzky-Golay smoothing and IBPLS models. Spectrosc. Spectr. Anal. 35 (6), 1529–1533.
Huang, Y.B., Ouellet-Plamondon, C.M., Thomson, S.J., 2017. Characterizing downwind drift deposition of aerially applied glyphosate using RbCl as tracer. Int. J. Agric. Biol. Eng. 10, 31–36.
Li, M., 2006. Spectral analysis technology and application. Science Press, Beijing, pp. 123–126.
Long, Q., Li, H.T., Zhang, Y.Y., Yao, S., 2015. Upconversion nanoparticle-based fluorescence resonance energy transfer assay for organophosphorus pesticides. Biosens. Bioelectron. 68, 168–174.
Melissa, A.K., Joe, D.L., Michael, P.S., 2015. Development and preliminary evaluation of a spray deposition sensing system for improving pesticide application. Sensor 15, 31965–31972.
Morey, N.S., Mehere, P.N., Hedaoo, K., 2017. Agriculture drone for fertilizers and pesticides spraying. Int. J. Eng. Appl. Technol. 3, 78–83.
Nuyttens, D., Baetens, K., Mde, S., Sonck, B., 2007. Effect of nozzle type, size and pressure on spray droplet characteristics. Biosyst. Eng. 97 (3), 333–345.
Salyani, M., Serdynski, J., 1990. Development of a sensor for spray deposition assessment. Trans. ASAE 33, 1464–1469.
Tang, Q., Chen, L.P., Zhang, R.R., Zhang, B., Yi, T.C., Xu, M., Xu, G., 2016. Atomization characteristics of normal flat fan nozzle and air induction nozzle under high speed airflow conditions. Trans. CSAE 32 (22), 121–128.
Tang, Y., Hou, C.J., Luo, S.M., Lin, J.T., Yang, Z., Huang, W.F., 2018. Effects of operation height and tree shape on droplet deposition in citrus trees using an unmanned aerial vehicle. Comput. Electron. Agric. 148, 1–7.
Tuck, C.R., Butler, M.C., Miller, P.C.H., 1997. Techniques for measurement of droplet size and velocity distributions in agricultural sprays. Crop Prot. 16 (7), 619–628.
Wang, C.L., He, X.K., Wang, X.N., Wang, Z.Z., Wang, S.L., Li, L.L., Jane, B., Andreas, H., Wang, Z.G., Mei, S.F., 2016. Distribution characteristics of pesticide application droplets deposition of unmanned aerial vehicle based on testing method of deposition quality balance. Trans. CSAE 32 (24), 89–97.
Wang, X.N., He, X.K., Wang, C.L., Wang, Z.Z., Li, L.L., Wang, S.L., Jane, B., Andreas, H., Wang, Z.G., 2017. Spray drift characteristics of fuel powered single-rotor UAV for plant protection. Trans. CSAE 33 (1), 117–123.
Xu, G.C., Xu, D.J., Xu, X.L., Sun, X.P., Gu, Z.Y., 2015. Pesticide droplets deposition and distribution in wheat field and its impact on control efficacy of small brown planthopper. Southwest China J. Agric. Sci. 28 (1), 140–145.
Xue, X., Lan, Y., Sun, Z., Chang, C., Hoffmann, W.C., 2016. Develop an unmanned aerial vehicle based automatic aerial spraying system. Comput. Electron. Agric. 128, 58–66.
Yang, S., Yang, X., Mo, J., 2017. The application of unmanned aircraft systems to plant protection in China. Prec. Agric. 21, 1–15.
Zhang, D.Y., Lan, Y.B., Wang, X., Zhou, X.G., Chen, L.P., Li, B., Ma, W., 2016. Assessment of aerial agrichemical spraying effect using moderate-resolution satellite imagery. Spectrosc. Spectr. Anal. 36 (6), 1971–1977.
Zhang, J., He, X.K., Song, J.L., Zeng, A.J., Liu, Y.J., Li, X.F., 2012. Influence of spraying parameters of unmanned aircraft on droplets deposition. Trans. Chinese Soc. Agric. Mach. 43 (12), 94–96.
Zhang, R.R., Chen, L.P., Lan, Y.B., Xu, G., Kan, J., Zhang, D.Y., 2014. Development of a deposit sensing system for aerial spraying application. Trans. Chinese Soc. Agric. Mach. 45 (8), 123–127.
Zhang, R.R., Wen, Y., Yi, T.C., Chen, L.P., Xu, G., 2017. Development and application of aerial spray droplets deposition performance measurement system based on spectral analysis technology. Trans. CSAE 33 (24), 80–87.
Zhou, L.P., He, Y., 2016. Simulation and optimization of multi spray factors in UAV. In: 2016 ASABE Annual International Meeting. St. Joseph, Mich., pp. 1–8.
Zhu, H., Salyani, M., Fox, R.D., 2011. A portable scanning system for evaluation of spray deposit distribution. Comput. Electron. Agric. 76, 38–43.